

L-Cysteine Functionalized Gold Nanocargos Potentiates Anti-HIV Activity of Azidothymidine against HIV-1_{Ba-L} Virus

Rohan Kesarkar*, Sailee Shroff, Madhuri Yeole and Abhay Chowdhary

Department of Virology, Haffkine Institute for Training Research & Testing, India

Submission: October 08, 2015; Published: October 17, 2015

*Corresponding author: Rohan Kesarkar, Department of Virology, Haffkine Institute for Training Research & Testing, Mumbai, MS, India, Tel: (+91) 7738997271; Email: rohannk27@gmail.com

Abstract

Gold nanoparticles (GNPs) stabilized with amino acid L-Cysteine were studied for their cytotoxicity, cell internalization and their ability as drug delivery cargos for increasing the efficacy of Azidothymidine (AZT) against HIV-1_{Ba-L} virus *in vitro*. GNPs exhibited low toxicity and increased cell internalization in peripheral blood mononuclear cells after conjugating with L-cysteine. CC₅₀ of GNPs was improved from 36.49ppm to 57.71ppm after functionalization with L-cysteine. GNP-Lcys demonstrated 70% drug carrying capacity and displayed a sustained drug release profile under physiological pH. GNPs were capable of halting HIV replication in both pre and post infection assays with an IC₅₀ value of 41.13ppm and 30.93ppm respectively. A statistically significant increase in anti-viral activity of AZT was seen (26.5% increment) (P<0.01) when it was conjugated to GNP-Lcys. Thus gold nanoparticles can be considered as an alternative anti-viral candidate as well as a potent drug delivery vehicle for improvising HIV therapeutics (Figure 1).

Keywords: Gold nanoparticles; CC₅₀; Endocytosis; Drug release kinetics; IC₅₀; HIV-1_{Ba-L}; AZT; T cells

Abbreviations: GNPs: Gold Nanoparticles; AZT: Azidothymidine; AIDS: Acquired Immune Deficiency Syndrome; CC₅₀: 50% Cytotoxic Concentration; HAART: Highly Active Anti-Retroviral Therapy; HIV: Human Immunodeficiency Virus; IC₅₀: 50% Inhibitory Concentration; IL-2: Interleukin-2; Lcys: L-cysteine; PBMCs: Peripheral Blood Mononuclear Cells; PHA-P: Phytohaemagglutinin-P; SPR: Surface Plasmon Resonance; TCID₅₀: 50% Tissue Culture Infectivity Dose.

Introduction

Since its inception in 1981, HIV has killed more than a quarter of a billion people in the past 25 years. An estimate 39 million people are infected with human immunodeficiency type-1 virus (HIV-1) worldwide [1,2]. There are more than 125,000 research articles related to HIV/AIDS that are catalogued in Pubmed database of the National library of medicine, but the knowledge about this almost intelligent virus remains incomplete, mosaic of understanding. Absence of an effective cure or a vaccine clearly defines HIV/AIDS as one of the most formidable public health issue of our generation. Antiretroviral therapy continues to be the mainstay for HIV treatment. Latest minimum three-drug-combination initiative of Highly Active Anti-Retroviral Therapy (HAART) though has managed to reduce HIV-1 disease morbidity and improved life expectancy, but is proving to no longer remain an obstacle for the HIV. HAART has been currently found to be associated with disadvantages such as adverse effects, reduced bioavailability, rapid clearance, emergence of drug resistance

viral strains, inconvenient dosage regimen and inability to provide a functional cure i.e. complete eradication of HIV from system [3-10].

Recent years have shown tremendous growth of research and applications in the field of nanoscience and nanotechnology [11]. Nanoparticles, particularly metallic nanoparticles like gold and silver nanoparticles are increasingly finding space in various diagnostic and therapeutic applications [12,13]. Gold nanoparticles (GNPs) have recently emerged as a promising drug delivery system (DDS) due to their facile synthesis, ease of functionalization, biocompatibility and inherent non-toxicity [14]. Apart from being widely used as a carrier system for various drug delivery systems, GNPs have also been found to have potent anti-microbial and anti-viral activities [15-18]. Some of the noteworthy properties of GNPs used as drug carriers are high stability, high carrier capacity, feasibility of incorporation of both hydrophilic and hydrophobic substances and likelihood of various routes of administration, including oral application and inhalation [19].

In this study, we try to explore GNPs as potent anti-viral and drug delivery systems for ferrying ART drugs for better management of HIV therapy. AZT was attached onto L-cysteine tagged GNPs and studied for change in its anti-HIV efficacy *in vitro*. Efforts were also taken to understand the cell internalization and drug release pattern of the nano-conjugate.

Experimental

Materials

HIV-1_{Ba-L} virus and reagents required for carrying out anti-HIV assay were provided as a generous gift from Dr. Suzanne Gartner, Dr. Mikulas Popovic and Dr. Robert Gallo through NIH AIDS Research and Reference Reagent Program, USA. Chloroauric acid, AZT, L-cysteine, MTT and all other chemical were purchased from Sigma Aldrich, USA. Glasswares for nanoparticles synthesis were washed with aqua regia and distilled water to remove traces of metal contaminants.

Methods

Synthesis of L-cysteine capped gold nanoparticles (GNPs-Lcys):

Procedure to orchestrate GNPs with L-cysteine was adopted from one of our previous studies [20] where L-cysteine was incorporated during the synthesis of GNPs. Briefly, 20µl of 0.5% L-cysteine was added to 10ml of 1% sodium citrate and kept stirring at 170°C on a magnetic hot plate stirrer. Upon boiling, Chloroauric acid (HAuCl₄) at a final concentration of 100ppm was added and kept stirring till initiation of color change. For comparative significance, a set of GNPs were synthesized by same procedure without the addition of L-cysteine.

Coating GNP-Lcys with AZT:

Here we report drug attachment at room temperature. 100µg/ml of AZT was added to 10ml of GNP-Lcys under closed environment and kept under continuous stirring for 4 hours. The concentration of AZT for coating onto GNP-Lcys was determined based upon optimization studies (data not shown) done in our laboratory to determine maximum concentration of drug attachment without affecting the stability of the nanoparticles.

Characteristic determination of GNP-Lcys and GNP-Lcys-AZT:

Preliminary characterization of nanoparticles and their conjugates was done by UV-visible spectroscopy using a dual beam Varian Cary UV-Vis spectrophotometer. Morphological features of GNPs were studied by Transmission electron microscope (TEM) (Zeiss Microimaging Gm bH, Germany). Attachment of drug onto GNPs was analyzed by fourier transformed infrared spectroscopy (Vertex 80, Bruker, Germany) and zeta potentials were calculated using Malvern Zetasizer (Brookhaven).

Toxicity and internalization of GNPs-Lcys:

For therapeutic applicability, toxicity of GNPs was inspected by tissue culture based MTT assay. Briefly, PBMCs were isolated by density gradient centrifugation using ficol as a density gradient [21]. PBMCs maintained in RPMI-1640 medium and supplemented with 10% (v/v) Fetal bovine serum were seeded

into 96 flat bottom well plates at concentration of 4x10⁵ cells/ml at 37°C and 5% CO₂. After 24 hours of incubation, medium was changed and different dilutions of blank GNP and GNP-L-Cys were added into wells respectively. After overnight incubation the cells were washed once with PBS and incubated with MTT dye (5mg/ml) for 4hrs at 37°C. After 4hrs of incubation, Dimethyl sulfoxide (DMSO) was added to each well and read at 570nm using a microplate reader (Biotek India Ltd.). Transition of colour change from yellow to purple is directly proportional to cellular mitochondrial metabolism and cell viability. Percentage cell toxicity was determined by following equation:

$$\text{Percent (\%)} \text{ Cell toxicity} = [(P - S) / P] \times 100 \dots (1)$$

Where, S = Sample reading and P = Positive control (only cells) reading. 50% cytotoxic concentration of nanoparticles synthesized (CC₅₀) was calculated by analyzing the above data using GRAPH PAD PRISM software, version 3.0.

Endocytosis is known to happen best at 37°C. Thus internalization of GNPs in PBMCs was studied with respect to temperature as parameter. Different concentrations of GNPs and GNP-Lcys below the CC₅₀ value were incubated at different time points (30min, 60min and 120min) with PBMCs in different 96 well flasks. One set of flask was incubated at 37°C while other flask was incubated at 4°C - an inhibitory temperature for endocytosis. After each time point, the supernatant was discarded and cells were washed twice with PBS to remove excess of GNPs that had not internalized. Cells were then digested with aqua regia (1 part HNO₃ and 3 parts of HCl) for 15 to 20 minutes. The samples were further diluted to a final volume of 5 ml in distilled water and 5% of HNO₃. The Au content in the samples was measured by inductively coupled plasma-atomic absorption spectroscopy (ICP-AES). Results obtained were converted into percentage concentration internalized. The results obtained were an average of three replicates from two independent experiments.

Drug kinetics of the nano-conjugate:

The GNP-Lcys-AZT conjugate was purified by extensive dialysis in nano-pure water for 1 hours using a dialysis membrane tube (MW cut-off of 3000 Da) to remove and quantitate the excess amount of unbound AZT. Drug loading efficiency onto GNPs was calculated using following equation:

$$\text{Drug loading efficiency} = \frac{\text{Total amount of drug loaded} - \text{Free drug}}{\text{Theoretical amount of drug loaded}} \times 100$$

To comprehend the drug release pattern, 5 ml of conjugate was sealed in a two different dialysis tubes and the entire system was kept at 37°C in 50 ml phosphate buffer solution at pH 7.2 under mild stirring. To measure the drug release content, 3 ml of sample was periodically removed and replaced with an equivalent volume of the phosphate buffer solution. The amount of released AZT was analyzed with spectrophotometer at 266nm. The experiments were performed in triplicate for each of the samples. The *in vitro* release data was finally related to various mathematical models like zero order, first order, Higuchi model etc. to predict the drug release mechanism and kinetics. Correlation coefficient (R) was calculated for each release model

and the best fit release model was selected with highest 'R' value [17].

Anti-HIV activity of GNPs and nano-conjugate:

Isolation and activation of peripheral blood mononuclear cells (PHA-PBMCs) and Drug susceptibility assay to determine the anti-viral activity of the conjugate was carried out as per standard protocols of division of AIDS National Institute of Allergy and Infectious Diseases, National Institutes of Health [18,22,23]. HIV is known to particularly infect T cells via CD4 receptor based assistance. For selective growth of T cells from the population of mononuclear cells and over-expression of surface markers like CD4, PBMCs were activated with phytohemagglutinin (PHA-P) and interleukin-2 (IL-2) for 24-72 hours prior to infection. To determine if GNPs possess anti-HIV activity, the assay was executed in a pre and post infection format. For pre-infection assay different dilutions of GNPs were incubated with 3×10^4 TCID₅₀ of HIV-1_{Ba-L} cell free virus for 1hour at 37°C and then allowed to infect activated PBMCs with 10⁻¹ multiplicity of infection. Whereas, for post infection assay, same amount of viral particles were first allowed to infect PBMCs followed by addition of different dilutions of GNPs. The concentrations of GNPs selected were less than the CC₅₀ values obtained from MTT assay. Anti-HIV activity of nano-drug conjugate was studied only by post infection protocol. HIV infection was assessed after 4 days of incubation by quantifying the viral p24 antigen by ELISA.

Statistical analysis:

All data were analyzed using the GraphPad Prism software (Version 3.0). Anti-viral experiment was repeated three times and the data were analyzed by Bonferroni's multiple comparison test. A P-value less than 0.05 considered statistically significant.

Results and Discussion

Synthesis of GNP-Lcys

Conversion of chloroauric acid into gold nanoparticles was seen as a transition in the solution from transparent to wine red color. Spectral measurements of GNPs demonstrated an intense peak between 500 to 550 nm (Figure 2) which is characteristic of GNPs and results due to surface Plasmon resonance (SPR) [24]. As compared to blank GNPs; Lcys functionalized GNPs displayed a decrease in peak intensity with a prominent blue shift from 528nm to 521nm (Figure 2). Blue shift in SPR is an indication of change in the surface chemistry of GNPs due to adsorption of L-cysteine. TEM images (Figure 3) confirmed synthesis of 40-50nm multifaceted cuboidal shaped nanoparticles. It can be postulated that incorporation of amino acid L-cysteine during synthesis might have resulted in stable aggregation of small spherical shaped GNPs due to Ostwald ripening, resulting into synthesis of large multifaceted cuboidal nano-structures at the expense of smaller ones. This method of incorporation of linker concurrent to synthesis produced highly stable nano-complex and can prove to be an easy and efficient method for functionalization of nanoparticles.

The infra-red spectrum of GNP-L-Cys was collected in the course of the reaction in the spectral range of 4000cm⁻¹ to 400cm⁻¹

¹. FTIR spectra of GNPs synthesized with L-cysteine (Figure 4a) showed presence of many peaks typical of L-cysteine. The most prominent peak was at 3434.69 cm⁻¹, which represents N-H stretch of primary and secondary amines. Mild peaks from 1243 – 1122 cm⁻¹ can be speculated to be of C-N stretch of aliphatic amines. Whereas, a narrow peak at 1629.04 cm⁻¹ correspond to the C=O stretch of carboxylic acid. Peaks at 2924 and 2853 cm⁻¹ suggests C-H stretch of alkanes while, a small peak cluster at 670cm⁻¹ represents the (=C-H) bend of alkanes. All these functional groups reveal presence of amine group (-NH₂) and carboxylic group (-COOH) of L-cysteine and confirm its incorporation onto the GNPs during the synthesis. The absence of thiol group at 2500cm⁻¹ suggests that the -SH group of L-cysteine has reacted with the gold during the formation of GNPs, rendering -NH₂ and -COOH groups free for further attachment of the drug onto GNPs.

Coating of AZT onto GNP-Lcys

Spectral observation of the conjugate after AZT attachment; showed an increase in the peak intensity with a red-shift of 3nm in wavelength (521nm to 524nm) as shown in the Figure 1. This could probably be due to the change in surface chemistry of the GNPs after impregnation with AZT. Zeta potential value showed a decrease in charge from -11.7mV to -15.21 mV after

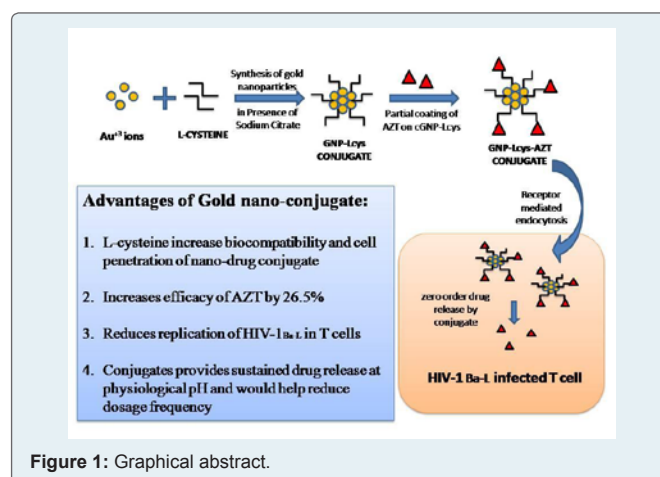


Figure 1: Graphical abstract.

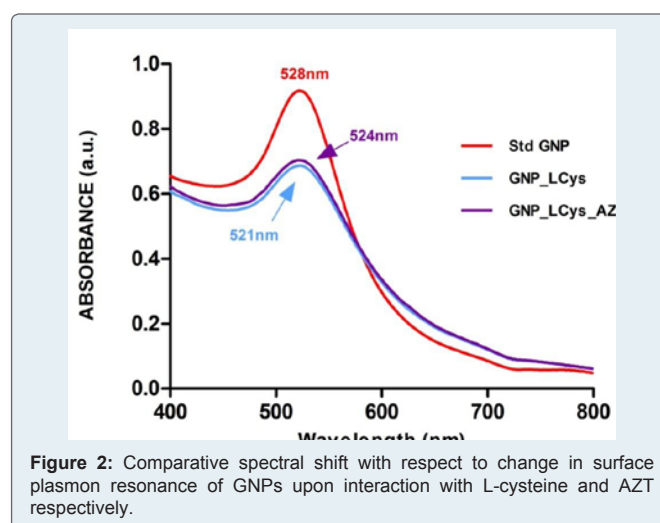


Figure 2: Comparative spectral shift with respect to change in surface plasmon resonance of GNPs upon interaction with L-cysteine and AZT respectively.

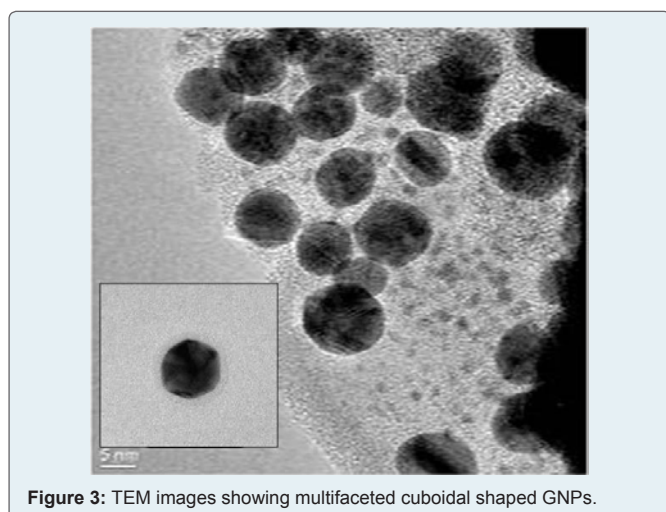


Figure 3: TEM images showing multifaceted cuboidal shaped GNPs.

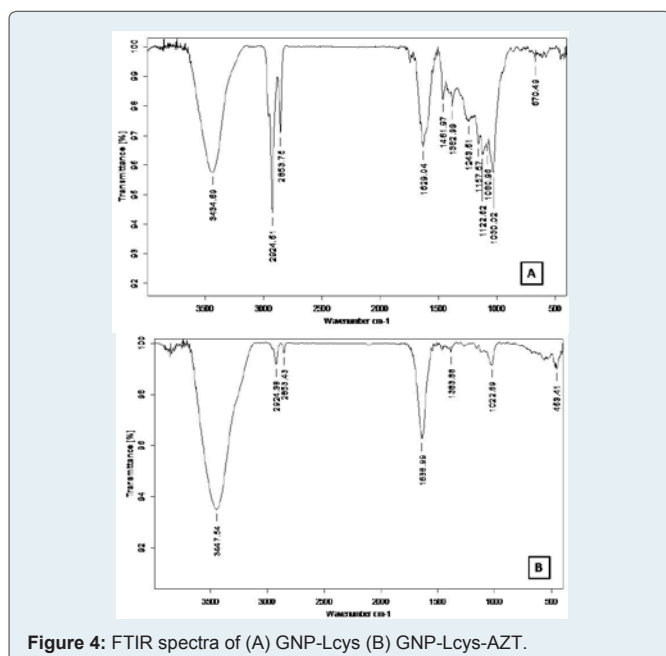


Figure 4: FTIR spectra of (A) GNP-Lcys (B) GNP-Lcys-AZT.

conjugation with AZT; thus suggesting adsorption of the drug onto the nanoparticles. Decrease in the zeta value could be due to the presence of benzene ring in the AZT. This explanation also undermines the possible interaction of the azide group of AZT with the nano-linker intermediate and decrease the positive charge in the system. The size of the gold nanoparticles- linker intermediate according to zeta measurements was further found to increase from 42.8nm to 71.52 nm after conjugation with AZT, which further confirms attachment of AZT onto GNPs.

FTIR spectrum of GNP-Lcys and GNP-Lcys-AZT was further compared to obtained a better understanding of attachment between the drug and nano-linker intermediate. IR-spectra of GNP-Lcys-AZT (Figure 4b) showed a peak shift of N-H stretch from 3434 to 3447 cm^{-1} . The spectra also showed a prominent peak shift of (C=O) carboxylic stretch from 1629 to 1638 cm^{-1} . Corresponding peaks from 1383 to 1022 cm^{-1} were also damped which represents C-O stretch. Emergence of peaks at 435 cm^{-1}

is typical of C-C stretch and suggests incorporation of aromatic groups of AZT. These spectral shifts suggest adsorption of AZT onto GNP-Lcys and involve interaction of amine group of L-Cysteine with the alcoholic group ($\text{CH}_2\text{-OH}$) of the sugar present in AZT. A decrease in peak transmittance corresponding to the azide group of AZT may be due to a negative induction effect of carboxylic group of the linker.

Drug release kinetics

In the process of designing an efficient carrier system for drug delivery, it is imperative that the candidate carries high amount of drug payload as well as provide control over its release to maintain the required therapeutic concentration in the system. From equation 2, percent drug loading efficiency of GNP-Lcys was found to be 70%. Such high amount of payload carrying capacity might be due to high surface to volume ratio of GNPs; making them favourable candidate for drug delivery system. Drug release studies at physiological pH demonstrated a constant concentration of drug released by the nano-conjugate w.r.t. time (Figure 5). Mathematical models applied to this data suggested that the GNP-Lcys-AZT conjugate followed zero order release kinetics. Zero order release kinetics highlights a constant drug release profile, where the amount of drug release is independent of the drug concentration loaded or left to be released and ideal for maintaining constant therapeutic concentration of the drug in circulation and prolonged pharmacological action.

Toxicity and internalization of GNPs

Percent cellular toxicity with respect to increase in log concentrations of blank GNPs and GNP-Lcys is shown in Figure 6. Both the nanoparticles displayed high cell survival at lower concentrations, which progressively worsened at higher concentrations. However, GNPs after functionalization with L-cysteine demonstrated higher CC_{50} values as compared to blank GNPs, suggesting that GNP-Lcys were more biocompatible than GNPs alone.

The initial contact and subsequent crossing of the nanoparticles through the cell membrane is a critical process that is expected to exert a profound effect on the cells and tissues. To study the effect of gold nanoparticle size and surface composition on cellular uptake, ICP-AES was employed to detect and quantify

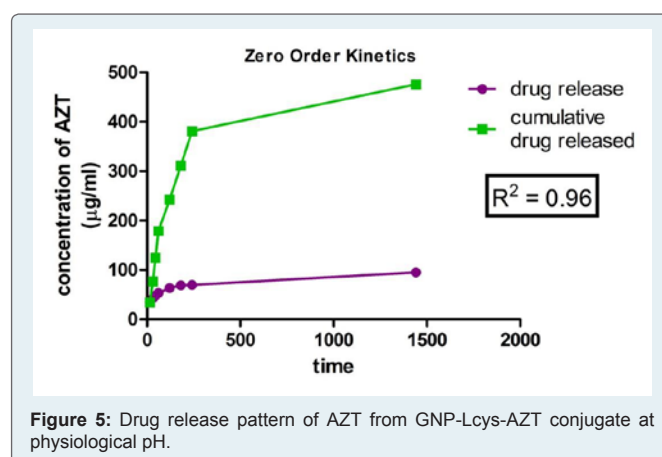


Figure 5: Drug release pattern of AZT from GNP-Lcys-AZT conjugate at physiological pH.

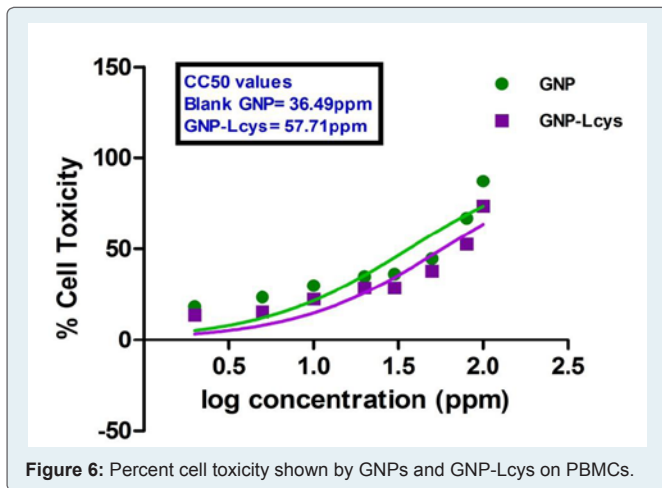


Figure 6: Percent cell toxicity shown by GNPs and GNP-Lcys on PBMCs.

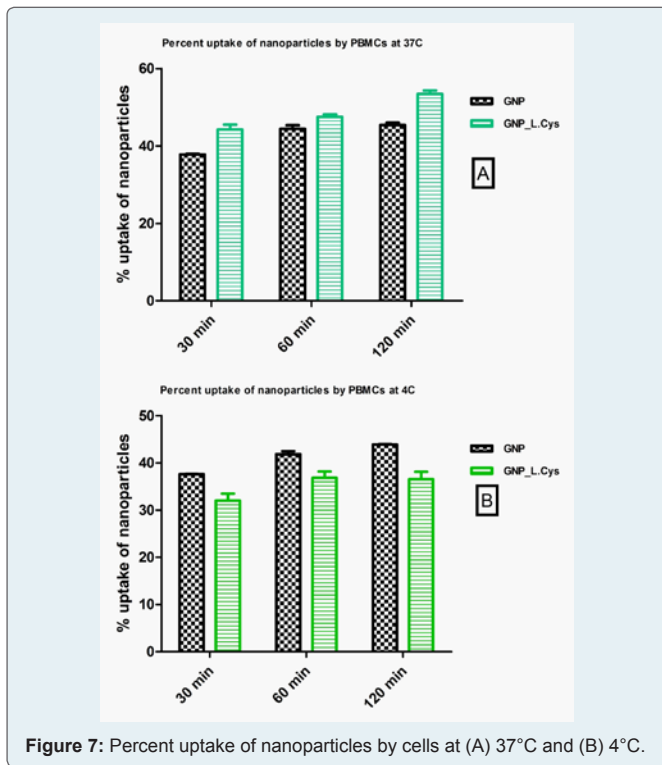


Figure 7: Percent uptake of nanoparticles by cells at (A) 37°C and (B) 4°C.

the intracellular Au content on PBMCs. Inductively coupled plasma atomic emission spectroscopy (ICP-AES), as compared to other imaging techniques, is a more sensitive and accurate method to quantify small amounts of gold nanoparticles within the cells. Nanoparticle uptake was also studied as a function of temperature. Numerous investigators have shown in many systems that endocytosis does not occur below 10°C [25]. Thus nanoparticle uptake was studied at two different temperatures i.e. 37°C and 4°C. As seen in Figure 7a & 7b, GNPs showed higher amount of cell internalization at 37°C as compared to 4°C. Thus GNPs preferentially follow receptor mediated endocytosis to enter cells. However, it was noticed that presence of L-cysteine onto GNPs increased the cellular uptake by 10%. Thus it can be concluded that L-cysteine increases the cell uptake profile of nanoparticle conjugate and might improve drug delivery.

Anti-HIV activity of GNPs and nano-conjugate

As shown in Figure 8a, GNPs showed increase in the antiviral activity with increasing concentrations for both pre and post-infection assay with an IC50 value of 41.13ppm and 30.93ppm respectively. The IC₅₀ values were calculated from the log-concentration-response curves using GRAPH PAD PRISM software, version 3.0. Thus gold nanoparticles were found to exert anti-HIV activity even at early stages of viral replication. It can be hypothesized that the exposed sulphur bearing residues of the glycoprotein knobs would be attractive sites for nanoparticle interaction. In case of GNPs, the anti-HIV activity might mainly be due to their polyanion surface which possesses the ability to bind to the positively charged amino acids in the V3 loop/second binding site of the viral envelope glycoprotein gp120. Post-entry inhibition studies revealed that gold nanoparticles (GNPs) have other sites of intervention on the viral life cycle, besides fusion or entry. Gold nanoparticles are known to complex with electron donating groups containing sulphur, oxygen or nitrogen that are generally present in thiols or phosphates in the amino acids and nucleic acid. Thus they are likely to inhibit post-entry stages of infection by blocking HIV-1 proteins other than gp120, like reverse transcriptase enzyme, proteases etc.

To assess if gold nanoparticles can act synergistically with the available anti-retrovirals, the synthesized nano-drug conjugate was subjected to drug-susceptibility assay. As the drug (AZT) used for conjugation act on the viral life cycle post viral entry, we performed the post-infection drug susceptibility assay to determine their activity. Comparative analysis revealed a noteworthy reduction in p24 antigen production in nano-conjugate challenged culture as compared to p24 levels in cultures challenged with AZT alone. From Figure 8b, a substantial 26.55% increase in activity was seen when AZT was fired with

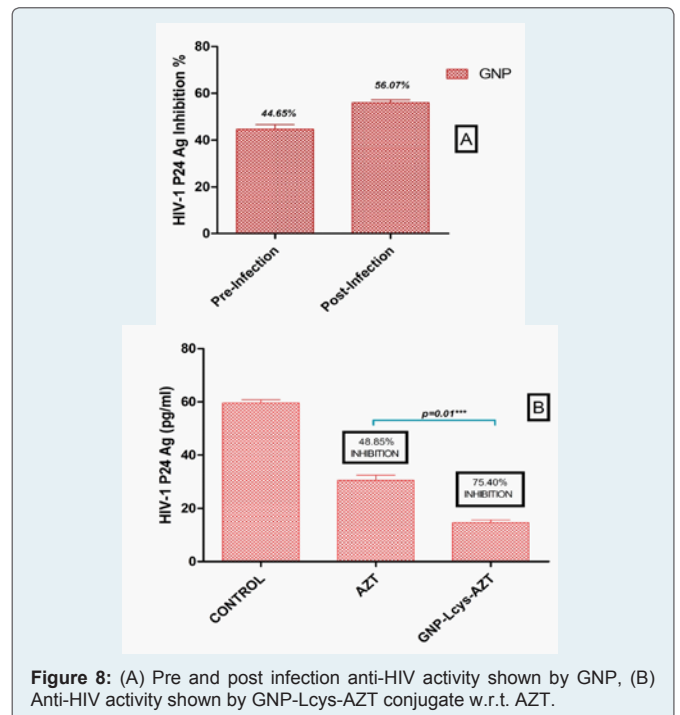


Figure 8: (A) Pre and post infection anti-HIV activity shown by GNP, (B) Anti-HIV activity shown by GNP-Lcys-AZT conjugate w.r.t. AZT.

GNP-Lcys. The results presented here demonstrate that the therapeutic efficacy of a molecule can be increased or improvised by conjugating them to gold nanoparticles.

Conclusion

An ideal retroviral agent should act directly on the virus along with acting on other replicating stages prior to integration of proviral cDNA. It should be absorbable by uninfected cells in order to provide a barrier to infection by residual active virus and be effective at non-cytotoxic concentration. Our gold nanoparticles were found to comply all these criteria's. Having such a varied panel of targets and showing both pre and post infection anti-HIV activities, along with improvising the efficacy of the conjugated drugs, gold nanoparticles can be possible alternative to currently available therapeutic management of HIV/AIDS.

Acknowledgements

The authors wish to acknowledge technical support from SAIF laboratory, IIT, Bombay and Tata Institute of Fundamental Research, Mumbai. We also thank Indian Council of Medical Research, Govt. of India for providing fellowship to the corresponding author.

Contribution of authors

Rohan Kesarkar: Designed, Performed and analyzed study and wrote paper.

Sailee Shroff and Madhuri Yeole: Performed study; particularly nanoparticle synthesis and collected data.

Abhay Chowdhary: Designed and analyzed study.

References

- Fauci AS (2003) HIV and AIDS: 20years of science. *Nat Med* 9(7): 839-843.
- Global report (2012) UNAIDS report on the global AIDS epidemic.
- Mamo T, Moseman EA, Kolishetti N, Salvador-Morales C, Shi J, et al. (2010) Emerging nanotechnology approaches for HIV/AIDS treatment and prevention. *Nanomedicine (Lond)* 5(2): 269-285.
- Buckheit RW, Watson KM, Morrow KM, Ham AS (2010) Development of topical microbicides to prevent the sexual transmission of HIV. *Antiviral Res* 85(1): 142-158.
- Pirrone V, Wigdahl B, Krebs FC (2011) The rise and fall of polyanionic inhibitors of the human immunodeficiency virus type 1. *Antiviral Res* 90(3): 168-182.
- Majid A, Redfield R, Gilliam B (2012) The use of preexposure prophylaxis treatments for HIV prophylaxis. *HIV/AIDS Res Palliative Care* 4: 17-28.
- Mahajan SD, Aalinkeel R, Law WC, Reynolds JL, Nair BB, et al. (2012) Anti-HIV-1 nanotherapeutics: promises and challenges for the future. *Int J Nanomedicine* 7: 5301-5314.
- Hankins CA, Dybul MR (2013) The promise of pre-exposure prophylaxis with antiretroviral drugs to prevent HIV transmission: a review. *Curr Opin HIV AIDS* 8(1): 50-58.
- Morris GC, Lacey CJ (2010) Microbicides and HIV prevention: lessons from the past, looking to the future. *Curr Opin Infect Dis* 23(1): 57-63.
- Potter SJ, Chew CB, Steain M, Dwyer DE, Saksena NK (2004) Obstacles to successful antiretroviral treatment of HIV-1 infection: problems & perspectives. *Indian J Med Res* 119(6): 217-237.
- Istrate CM (2014) Interaction of functionalized nanoparticles with cell membranes. *Biointerface Res Appl Chem* 4(6): 895-901.
- Sanvicens N, Marco MP (2008) Multifunctional nanoparticles-properties and prospects for their use in human medicine. *Trends Biotechnol* 26(8): 425-433.
- Fabio S, Catherine D, Paolo C, Patrick C (2005) Metallic colloid nanotechnology, applications in Diagnosis and therapeutics. *Curr Pharm Des* 11(16): 2095-2105.
- Kim CK, Ghosh P, Rotello VM (2009) Multimodal drug delivery using gold nanoparticles. *Nanoscale* 1(1): 61-67.
- Vijayakumar S, Ganesan S (2012) Gold nanoparticles as an HIV entry inhibitor. *Curr HIV Res* 10(8): 643-646.
- Zhou Y, Kong Y, Kundu S, Cirillo J, Liang H (2012) Antibacterial activities of gold and silver nanoparticles against *Escherchia coli* and *bacillus Calmetter-Guerin*. *J Nanobiotechnology* 10: 19.
- Kesarkar R, Sangar V, Oza G, Sawant T, Kothari S, et al. (2014) Synthesis, characterization and hepartoprotective activity of neem gold nanoparticles for improved efficacy and sustained drug release profile of Azidothymidine. *Int J Pharm Sci Rev Res* 26(2): 117-122.
- Kesarkar R, Oza G, Pandey S, Dahake R, Mukherjee S, et al. (2012) Gold nanoparticles: effective as both entry inhibitors and virus neutralizing agents against HIV. *J Microbiol Biotech Res* 2(2): 276-283.
- Gelperina S, Kisich KO, Iseman MD, Heifets L (2006) The potential advantages of nanoparticles drug delivery systems in chemotherapy of tuberculosis. *Am J Respir Crit Care Med* 172(12): 1487-1490.
- Kesarkar R, Yeole M, Dalvi B, Sharon M, Chowdhary A (2015) Simplistic approach towards synthesis of highly stable and biocompatible L-cysteine capped gold nanospheres intermediate for drug conjugation. *Int J Pharm Sci Rev Res* 31(1): 143-146.
- English D, Andersen BR (1974) Single step separation of red blood cells. Granulocytes and mononuclear leukocytes on discontinuous density gradients of ficol-Hypaque. *J Immunol Methods* 5(3): 249-252.
- National Institute of Allergy and Infectious Diseases (1997) (U.S.) Division of AIDS, National Institutes of Health (U.S.), DAIDS Virology Manual for HIV Laboratories, National Institute of Allergy and Infectious Diseases, Division of AIDS 78-91.
- Nakata H, Steinburg SM, Koh Y, Maeda K, Takaoka Y, et al. (2008) Potent Synergistic Anti-Human Immunodeficiency Virus (HIV) Effects Using Combinations of the CCR5 Inhibitor Aplaviroc with Other Anti-HIV Drugs. *Antimicrob Agents Chemother* 52(6): 2111-2119.
- Wolfgang H, Nguyen TKT, Aveyard J, Fernig DG (2007) Determination of size and concentration of gold nanoparticles from UV-vis Spectra. *Anal Chem* 79(11): 4215-4221.
- Freese C, Uboldi C, Gibson MI, Unger RE, Weksler BB, et al. (2012) Uptake and cytotoxicity of citrate-coated gold nanospheres: Comparative studies on human endothelial and epithelial cells. *Part Fibre Toxicol* 9: 23.